JOURNAL OF GEOPHYSICAL RESEARCH, VOL. 86, NO. C11, PAGES 11,065–11,072, NOVEMBER 20, 1981

On the Dynamics of the Ice Sheets

P. HALFAR

Max-Planck-Institut für Meteorologie, Hamburg, Federal Republic of Germany

A similarity solution of the equation that describes the time evolution of an ice sheet is obtained by separation of variables. It describes the motion of an initial δ function ice sheet distribution and is asymptotically stable with respect to all perturbations that leave the total volume invariant. Homogeneity in one horizontal direction is assumed.

1. INTRODUCTION

On time scales larger than 10^3 years, the motion of the ice sheets plays an important role in the climatic system of the earth. To explain these variations, two mechanisms have mainly been discussed. One is the external forcing via the orbital parameters of the earth [*Hays et al.,* 1976]. There is good evidence that the obliquity of the earth's axis and the precession of the equinoxes influence the ice sheet variations. However, a physical connection between the large 10^5 years peak in the climatic spectrum and the period of eccentricity of the earth's orbit remains doubtful [*Rooth et al.,* 1978]. The other mechanism is a feedback between the variables of the climatic system [*Imbrie and Imbrie,* 1980; *Källen et al.,* 1979; *Oerlemans,* 1979]. The aim of such feedback models is to find an eigenmode with a characteristic time scale of 10^5 years.

It is important for any model of ice sheet dynamics to master the simplest case when external forcing and feedback mechanisms are absent. Therefore, I shall consider only that part of the motion of an ice sheet that is due to the flow law of the ice. A two-dimensional case is treated (length and height). The ice is assumed to rest on a flat ground where the velocities vanish. It has not yet been realized that the nonlinear equation, which describes in the small slope approximation the time evolution of the surface [*Mahaffy,* 1976], has a similarity solution of finite extent that grows in length and shrinks in height. By linearizing the equation of motion around the similarity solution, any deviation from this solution which leaves the volume invariant can be shown to fade away in the course of time (i.e., this solution is asymptotically stable). The eigenvalues and eigenfunctions of the equation of motion that are linearized in the deviation are represented through standard analytical expressions. The result suggests that any solution of the equation of motion approaches during its time evolution a similarity solution.

The linearization around a given solution fits into the general scheme developed by Nye [*Paterson,* 1969] and *Weertman* [1958] in which the authors consider expansions around solutions, which are in equilibrium with sources and sinks, but the sawtooth pattern of isotopic records [*Rooth et al.,* 1978] indicates that the ice age ice sheets were far from equilibrium.

I hope that the similarity solution will also be useful to describe some of the more realistic cases when accumulation and ablation change the volume, sliding occurs on the bed, temperature varies in space and time, or ice-ocean interaction takes place along the marine margins of the ice sheet. If the internal friction of the ice that is responsible for the asymptotic stability of the similarity solution dominates some of these effects, then an expansion around similarity solutions might be valuable. As this task goes beyond the present paper, let me sketch how it could be done.

The above-mentioned more realistic properties add as perturbations to the equation of motion. At every time a solution of this perturbed equation can be approximated through a similarity solution by adjustment of volume, center of mass and length. The remaining difference is expanded in terms of the eigenfunctions of the unperturbed and in the deviations from this similarity solution linearized equation of motion. The three lowest modes do not occur, for these degrees of freedom are already fixed by adjustment of volume, center of mass, and length (cf. section 7). The perturbed equation is then linearized in the amplitudes of the higher eigenfunctions and yields a first-order differential equation for the time evolution of volume, center of mass, length, and these amplitudes. If the damping of these amplitudes, which is already there in the unperturbed case, is large compared with the perturbations, then they will remain small, the first-order expansion remains valid, and, therefore, the procedure is self-consistent. To repeat the essential assumption, the damping of deviations from the shapes of the similarity solutions that is caused by internal friction limits their growth, which is due to the perturbations.

In this way the model could consider all degrees of freedom of an ice sheet, and only a few of the lowest ones must be taken into account owing to the stronger damping of the higher modes that would save a lot of computer time. On the other hand, there would be more than 1 degree of freedom, which is necessary to build feedback models with cyclic motions. This would be a difference to the *Weertman* [1964] model, which has only the length as degree of freedom.

2. THE MODEL

Consider a two-dimensional ice sheet resting on a flat ground (Figure 1). Its motion is determined by Glen's flow law of the ice that connects the second invariants of the deviatoric stress tensor and the strain-rate tensor [*Nye,* 1957]:

$$\dot{\varepsilon} = \left(\frac{\sigma'}{A}\right)^n \tag{1}$$

and by the boundary condition of vanishing velocity on the bed. Neglecting longitudinal stress gradients, the vertically integrated equation of motion becomes in the small slope approximation [*Mahaffy,* 1976]

$$\frac{\partial h}{\partial t} = \frac{2}{(n+2)}\left(\frac{\rho g}{A}\right)^n \frac{\partial}{\partial x}\left(\frac{\partial h}{\partial x}\left|\frac{\partial h}{\partial x}\right|^{n-1} h^{n+2}\right) \tag{2}$$

Paper number 1C1095.
0148-0227/81/001C-1095$01.00

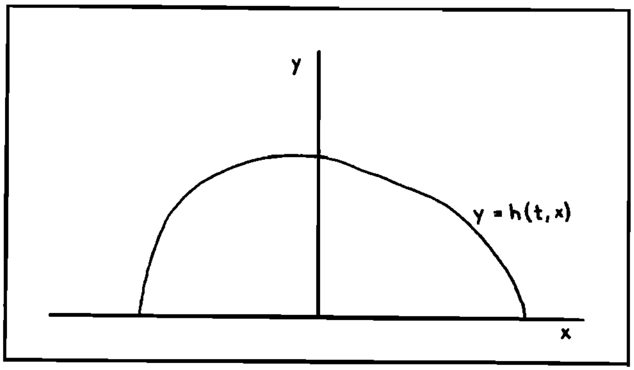

Fig. 1. Surface height versus horizontal distance of an ice cap.

where ρ is the density of the ice and g the acceleration of gravity. This equation agrees up to lowest order in the slope h_x, with *Nye*'s [1952] results.

Introducing dimensionless variables

$$\begin{aligned} t &\rightarrow t \cdot T \\ x &\rightarrow x \cdot L \\ h &\rightarrow h \cdot L \end{aligned} \tag{3}$$

where the time and length scales are

$$L[m] = \frac{1}{\rho g\,[\mathrm{bar} \cdot m^{-1}]} \simeq 11 \tag{4}$$

$$T\,[\mathrm{yr}] = \frac{n+2}{2} A^n\,[\mathrm{bar}^n \cdot \mathrm{yr}] \tag{5}$$

the equation (2) becomes

$$\frac{\partial h}{\partial t} = \frac{\partial}{\partial x}\left(\frac{\partial h}{\partial x}\left|\frac{\partial h}{\partial x}\right|^{n-1} h^{n+2}\right) \tag{6}$$

Typical values for A^n [bar$^n \cdot$ yr], which is also denoted by β^{-1} in the literature [*Andrews,* 1975], are

Temperature, °C	A^n [bar$^n \cdot$ yr]
0	6.06
−5	18.5
−10	58.8
−20	666

The exponent n in Glen's law is about 3.

In the neighborhood of the ice edge (6) is not valid as the surface slope becomes large. In the following this effect is neglected. If this neighborhood is small compared with the extension of the ice sheet, then the corresponding error should remain small too. The behavior of a glacier near its edge has been considered by *Nye* [1967].

3. A Similarity Ice Cap Solution

To solve (6), I make the separation assumption

$$h(t, x) = \sqrt{aV} f(t) g\left(\frac{x f(t)}{\sqrt{aV}}\right) \tag{7}$$

where V is the total volume. If g is a solution of finite extent, then it is always possible to choose $f(t)$ and a such that

$$g(0) = 1 \qquad g(1) = 0 \tag{8}$$

Substituting (7) in (6), the separated equations become

$$\frac{f'(t)}{f^{3n+3}(t)} = (aV)^{n/2}\, \frac{d/d\eta\,(g'(\eta)|g'(\eta)|^{n-1}\, g^{n+2}(\eta))}{d/d\eta\,(\eta g(\eta))} = c \tag{9}$$

where c is a constant and

$$\eta = \frac{x f(t)}{\sqrt{aV}} \tag{10}$$

The solution of (9) which satisfies (8) is

$$g(\eta) = (1 - |\eta|^{(1+n)/n})^{n/(2n+1)} \qquad |\eta| < 1 \tag{11}$$

$$f(t) = \left(\frac{t}{\tau_0}\right)^{-1/(3n+2)} \tag{12}$$

$$\tau_0 = \frac{1}{(3n+2)}\left(\frac{2n+1}{n+1}\right)^n (aV)^{-n/2} \tag{13}$$

$$a = \left(\frac{n+1}{2n}\right) \frac{\Gamma((5n^2+5n+1)/(n+1)(2n+1))}{\Gamma(n/(n+1))\,\Gamma((3n+1)/(2n+1))} \tag{14}$$

The meaning of (7) and (10) is a time dependent rescaling of height and length with scaling factor $\propto f(t)$, respectively, $\propto f^{-1}(t)$ such that the rescaled solution $g(\eta)$ extends from $\eta = -1$ to $\eta = +1$ and has maximal height $g(0) = 1$. Figure 2 shows a plot of this rescaled solution for the case $n = 3$.

In the perfect plasticity limit $n \rightarrow \infty$, Orowan's solution [*Weertman,* 1964] is obtained from the similarity solution. With the notation of *Weertman* [1964] the flow law (1) reads

$$\dot{\varepsilon} = C\left(\frac{\tau}{\tau_0}\right)^n \tag{15}$$

that is,

$$A^n = \tau_0^{\,n} \cdot C^{-1} \tag{16}$$

Calculating the limit of $f(t)$ at a fixed time, one has to consider (3) and (5). Therefore, the correct limit f_∞ is given by

$$f_\infty = \lim_{n\rightarrow\infty} f\left(\frac{t}{T}\right)\Bigg|_{t\ \mathrm{fixed}} \tag{17}$$

and equal to (cf. (5), (12), (13), (16))

$$f_\infty = (2\tau_0\,[\mathrm{bar}])^{1/3}\,(a_\infty V)^{-1/6} \tag{18}$$

where

$$a_\infty = \lim_{n\rightarrow\infty} a = \frac{3}{4} \tag{19}$$

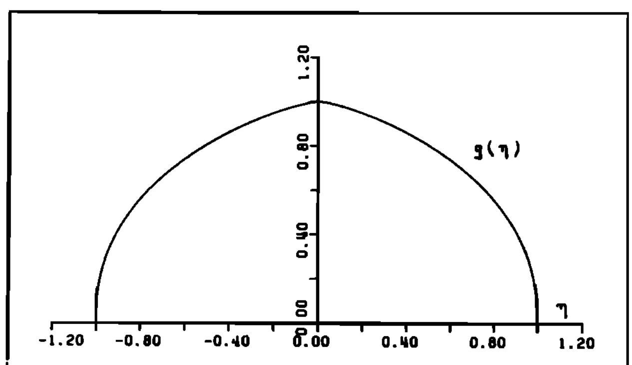

Fig. 2. $g(\eta)$ versus η for $n = 3$.

setting $1 = \eta = R\, f_\infty / \sqrt{a_\infty V}$ yields the half width

$$R = \sqrt{a_\infty V} \cdot f_\infty^{-1} \tag{20}$$

and considering (7) and (8) yields the maximal height

$$H = \sqrt{a_\infty V} \cdot f_\infty \tag{21}$$

Eliminating $a_\infty V$ and f_∞ from (18), (20), and (21) and reintroducing the true height and half width (cf. (3) and (4))

$$\begin{aligned} H &\rightarrow H \cdot \rho g[\text{bar}] \\ R &\rightarrow R \cdot \rho g[\text{bar}] \end{aligned} \tag{22}$$

the relation

$$H = \left(\frac{2\tau_0 R}{\rho g}\right)^{1/2} \tag{23}$$

between true height H and true half width R is obtained. The surface profile (11) becomes parabolic.

$$g_\infty(\eta) = \lim_{n\rightarrow\infty} g(\eta) = (1 - |\eta|)^{1/2} \tag{24}$$

The last two equations agree with Orowan's result [*Weertman*, 1964].

4. A Characteristic Time Scale

Consider an ice mass of volume V that is concentrated at one point in space. The time t, which this ice mass needs to increase its length to a value of $2R$, can be calculated from (10) and (12)–(14) by putting $1 = \eta = Rf(t)/\sqrt{aV}$ to

$$t = \frac{1}{(3n+2)}\left(\frac{2n+1}{n+1}\right)^n \frac{R^{3n+2}}{(aV)^{2n+1}} \tag{25}$$

Assume a volume that is equivalent to a cap of length $2R$ = 1000 km and height 1 km. By using (3)–(5) for $n = 3$ and temperature = 0° C leads to a time of 614000 years.

This result is not in contradiction to experimental data as (25) is very sensitive to changes in V and R (e.g., in the case $n = 3$ a change of a factor of 2 in the length at constant volume changes this time by a factor of $2^{11} = 2048$). It is therefore difficult to relate these time scales with time scales of past ice sheet variations.

To get a feeling for this result, consider the perfect plasticity limit $n \rightarrow \infty$. For a length of 2000 km and a shear stress of τ_0 of 1 to 0.5 bar the height is 4.8 to 3.4 km [*Weertman*, 1964]. Remembering that the height is porportional to the square root of the length, the above-used length of 1000 km requires a height of 3.4 to 2.4 km in the perfect plasticity case. The assumed height of 1 km belongs to a shear stress lower than τ_0, and therefore the flow essentially stops which explains the large time scale of 614000 years in the case $n = 3$.

5. Linearization of the Equation of Motion

I consider any solution h of (6) which is in the vicinity of the similarity solution (11)–(14). It is useful for the perturbation theory around this solution to define a function G by

$$h = \sqrt{aV}\, f(t) G(t, \eta) \tag{26}$$

V, η, a, and f are as in section 3. Equation (26) represents a rescaling such that the reference solution has half length and

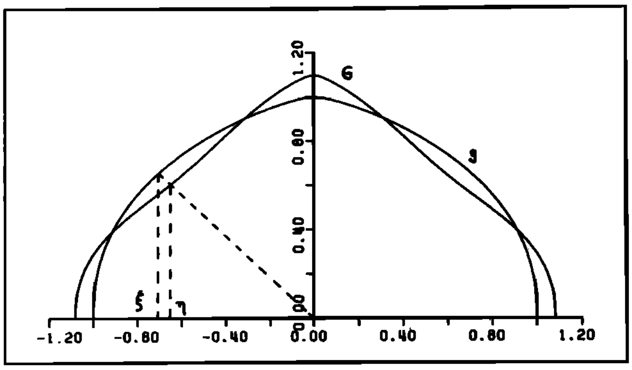

Fig. 3. Plots of $G(\eta)$ and $g(\eta)$ versus η and geometrical interpretation of the relation between η and ξ.

height equal to 1. Insertion in to (6) yields

$$t\frac{\partial G}{\partial t} = \frac{1}{3n+2}\frac{\partial}{\partial \eta}\left(\eta G + \left(\frac{2n+1}{n+1}\right)^n \frac{\partial G}{\partial \eta}\left|\frac{\partial G}{\partial \eta}\right|^{n-1} G^{n+2}\right) \tag{27}$$

Here $\partial/\partial t$, $\partial/\partial\eta$ denote differentiation for fixed η resp. t. Of course the similarity solution $G(t, \eta) = g(\eta)$ solves (27).

In linear perturbation theory, G is to be considered as g plus a small perturbation. For the following it is useful to consider simultaneously a perturbation of g and of the horizontal variable η (cf. Figure 3):

$$\eta = [1 + \varepsilon(t, \xi)]\xi \tag{28}$$

$$G(t, \eta) = [1 + \varepsilon(t, \xi)]g(\xi) \tag{29}$$

Usually a point of the perturbed solution is determined by an expansion around a reference point with the same horizontal coordinate. However, the reference solution is a distribution which is bounded in horizontal direction with vertical tangents at the boundary and the expansions up to first order around reference points, which are on or outside the boundary are not meaningful. The representation (28) and (29) avoids this difficulty by relating any point with nonvanishing height of the perturbed solution to a point with nonvanishing height of the reference solution such that the boundaries match.

An expansion of (27) up to first order in ε yields (cf. Appendix 1)

$$t\frac{\partial}{\partial t}\varepsilon = \mathscr{L}\varepsilon \tag{30}$$

where $\mathscr{L}$ is a linear differential operator and $\partial/\partial t$ denotes differentiation with ξ fixed. To guarantee the regularity of (28) and (29) one has to require (cf. Appendix 1)

$$\left|\frac{\partial}{\partial \xi}(\xi\varepsilon)\right| < 1 \tag{31}$$

6. Spectral Analysis

The eigenfunctions of $\mathscr{L}$ under the boundary condition (31) and the corresponding eigenvalues are calculated in Appendix 2. The functions are either symmetric (s) or antisymmetric (a) with respect to ξ,

$$\varepsilon_{s,k} = \frac{1}{\left(1 - z\dfrac{n}{2n+1}\right)} F\left(\frac{n^2-n-1}{(n+1)(2n+1)} + k, -k, \frac{n}{n+1}; z\right) \tag{32}$$

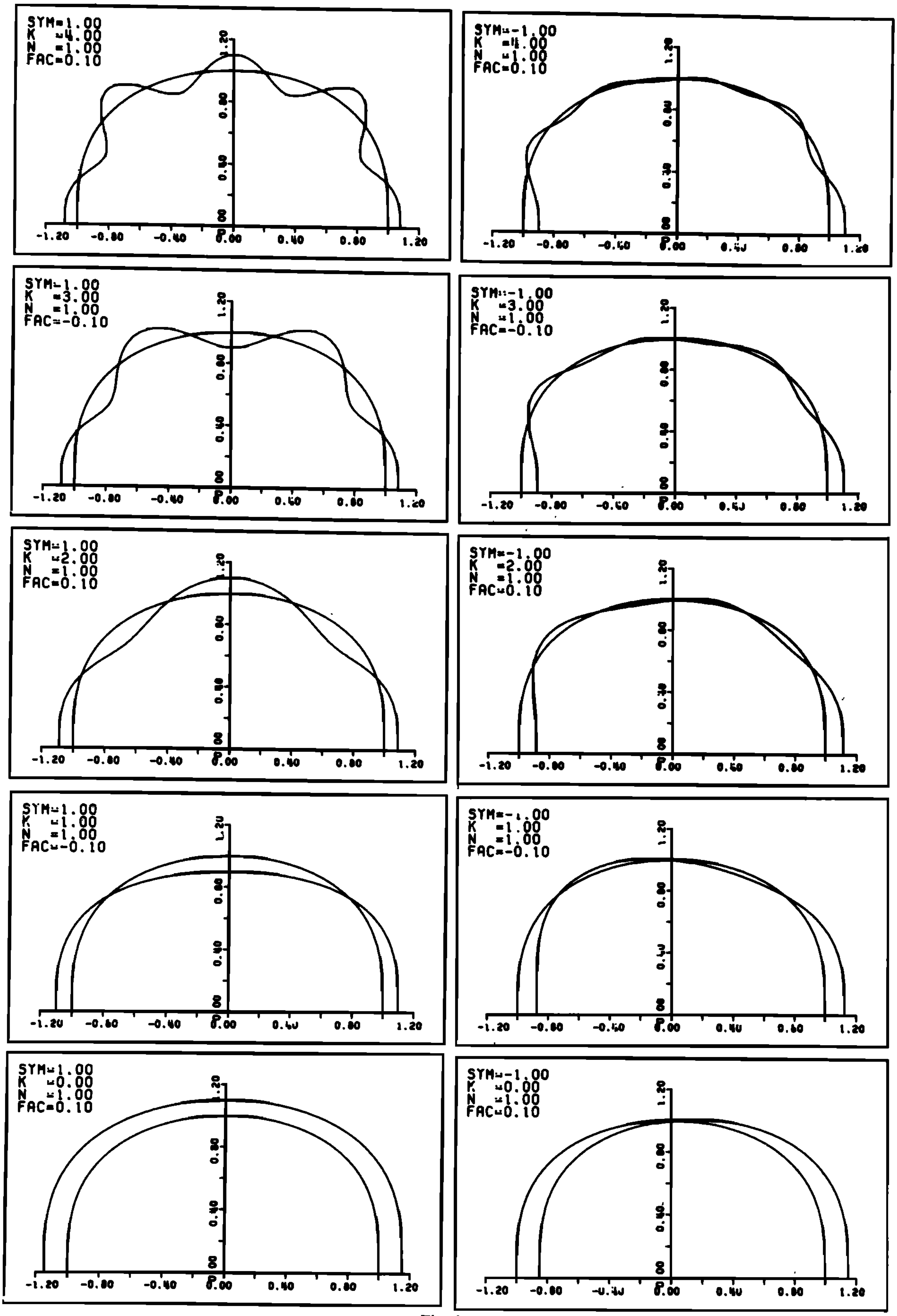

Fig. 4*a*

Fig. 4. Plots of the similarity solution and of deviations from it which represent eigenfunctions of the linearized equation of motion, where length and height are rescaled by time dependent factors such that the rescaled similarity solution becomes constant in time, extends from −1 to +1 in horizontal direction, and has maximal height 1. SYM = ±1 corresponds to the symmetric and antisymmetric case, respectively, and K (=k) = 0 ··· 4 denotes the number of the eigenfunction. (*a*) N (=n) = 1 which describes a Newtonian fluid; (*b*) N = 3 is the generally accepted value for the exponent in Glen's flow law. The eigenfunctions are unique up to an arbitrary factor FAC which is chosen to achieve amplitudes of suitable height for the figures.

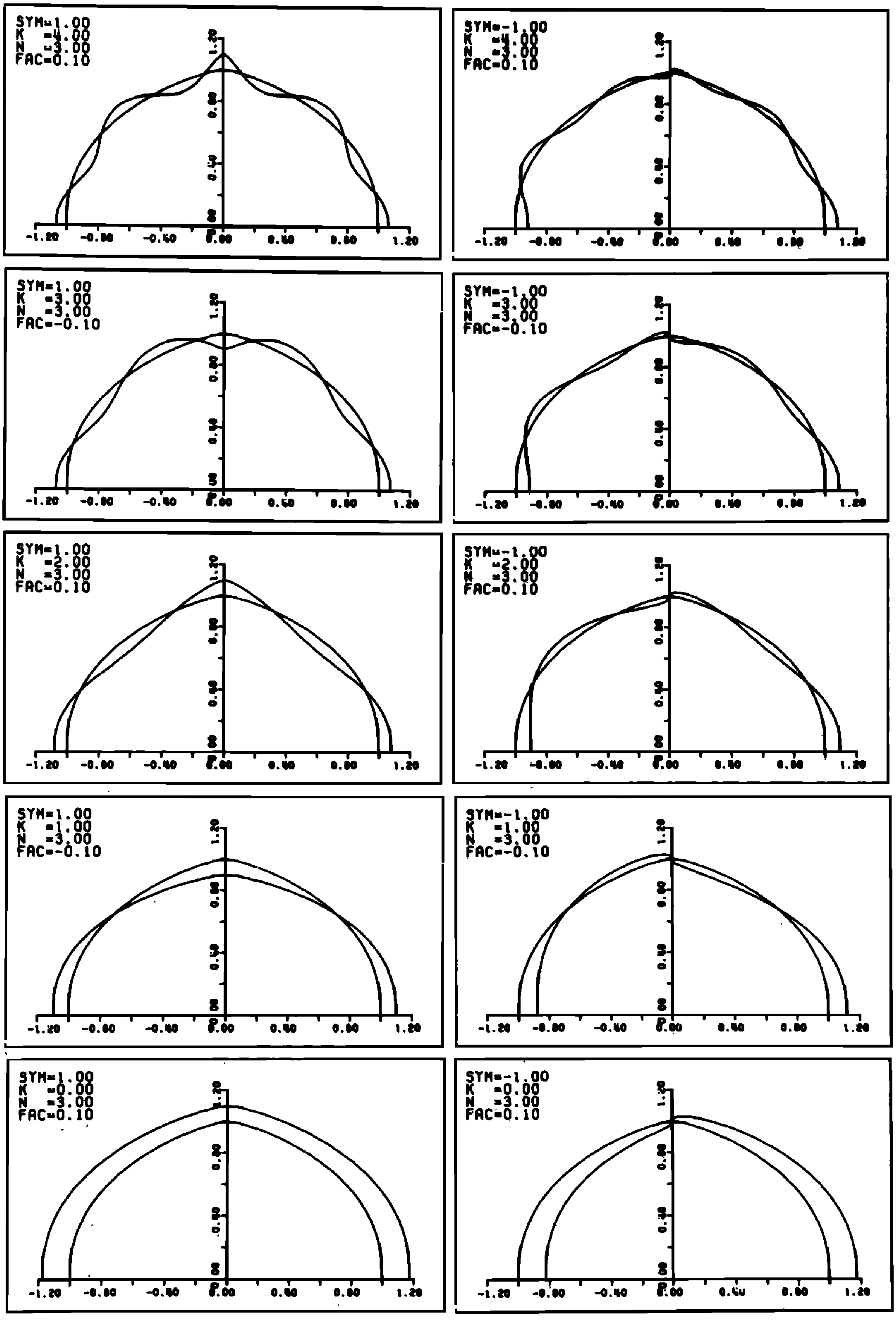
SYM=1.00
K =4.00
N =3.00
FAC=0.10
SYM=-1.00
K =4.00
N =3.00
FAC=0.10
SYM=1.00
K =3.00
N =3.00
FAC=-0.10
SYM=-1.00
K =3.00
N =3.00
FAC=-0.10
SYM=1.00
K =2.00
N =3.00
FAC=0.10
SYM=-1.00
K =2.00
N =3.00
FAC=0.10
SYM=1.00
K =1.00
N =3.00
FAC=-0.10
SYM=-1.00
K =1.00
N =3.00
FAC=-0.10
SYM=1.00
K =0.00
N =3.00
FAC=0.10
SYM=-1.00
K =0.00
N =3.00
FAC=0.10

Fig. 4*b*

$$\varepsilon_{a,k} = \frac{z^{1/n+1}}{\left[1 - z\dfrac{n}{2n+1}\right]} F\left[\frac{n^2+3n+1}{(n+1)(2n+1)} + k, -k, \frac{n+2}{n+1}; z\right] \tag{33}$$

$$z = \xi^{(1+n)/n} \qquad 0 < \xi < 1$$
$$k = 0, 1, 2 \cdots \tag{34}$$

where $F(a, b, c; z)$ is the Hypergeometric Function [*Smirnow*, 1970]. The corresponding eigenvalues of $\mathscr{L}$ are

$$\mu_{s,k} = -\frac{(n+1)(2n+1)}{n(3n+2)} k \left[k + \frac{n^2-n-1}{(n+1)(2n+1)}\right] \tag{35}$$

$$\mu_{a,k} = -\frac{(n+1)(2n+1)}{n(3n+2)} \left[k + \frac{n}{2n+1}\right]\left[k + \frac{1}{n+1}\right] \tag{36}$$

The time evolution of the eigenmodes is then (cf. (30)):

$$\varepsilon = \left[\frac{t}{\tau_0}\right]^{\mu_{s,k}} \cdot \varepsilon_{s,k} \tag{37}$$

$$\varepsilon = \left[\frac{t}{\tau_0}\right]^{\mu_{a,k}} \cdot \varepsilon_{a,k} \tag{38}$$

Figure 4 shows plots of the similarity solution and of deviations from it that represent eigenfunctions of the linearized equation of motion.

7. DISCUSSION

All eigenvalues of $\mathscr{L}$ except the first, which is zero, are negative and have been ordered in the sequence

$$\cdots \mu_{a,1} < \mu_{s,1} < \mu_{a,0} < \mu_{s,0} = 0 \tag{39}$$

Therefore, all the excitations, except the lowest one, approach zero as time approaches infinity. Since the volume of these excitations must then also approach zero, this is compatible with the conservation of the total volume only if the volume of all eigenmodes except the first one vanishes, which is indeed the case. This implies that the ice cap solution is asymptotically stable with respect to all perturbations that leave the total volume invariant.

The three lowest modes can be generated from the ice cap solution (7) and (11)–(14) by infinitesimal displacements in volume, space and time, respectively. They are displayed in Figure 4.

To find a measure for the decrease of the eigenmodes during their time evolution, the relative change $d\varepsilon/\varepsilon$ can be related to the relative change dR/R of the cap's half length R. Putting $1 = \eta = Rf(t)/\sqrt{aV}$ equation (12) yields

$$\frac{dR}{R} = -\frac{df}{f} = \frac{1}{(3n+2)}\frac{dt}{t} \tag{40}$$

and thus (cf. (30))

$$\frac{R}{\varepsilon}\frac{\partial\varepsilon}{\partial R} = (3n+2)\frac{t}{\varepsilon}\frac{\partial\varepsilon}{\partial t} = (3n+2)\frac{\mathscr{L}\varepsilon}{\varepsilon} \tag{41}$$

If μ is the eigenvalue of ε then the relative decrease $-d\varepsilon/\varepsilon$ is $-(3n+2)\mu$ times larger than the relative increase dR/R of the half length R. This ratio is given below for the three lowest modes.

Mode Number	$-(3n+2)\mu$
$s, k = 0$	0
$a, k = 0$	1
$s, k = 1$	$3n + 2$

In the case $n = 3$, the relative decrease of the third mode is already 11 times larger than the relative increase of the cap's length. For higher mode numbers k, this factor grows roughly with the square of k (cf. (35) and (36)).

The Hypergeometric Functions occurring in (32) and (33) are proportional to the Jacobi polynomials $G_k(p, q, z)$ [*Abramowitz and Stegun*, 1970], where

Symmetric case

$$p = \frac{(n^2-n-1)}{(n+1)(2n+1)} \qquad q = \frac{n}{(n+1)} \tag{42}$$

Antisymmetric case

$$p = \frac{(n^2+3n+1)}{(n+1)(2n+1)} \qquad q = \frac{(n+2)}{(n+1)} \tag{43}$$

They are orthogonal with respect to the weight function

$$w(z) = (1-z)^{p-q}z^{q-1} \tag{44}$$

and can be normalized

$$u_k = h_k^{-1/2}G_k \tag{45}$$

$$\int_0^1 dz\, w(z)u_l(z)u_k(z) = \delta_{l,k} \tag{46}$$

where

$$h_k = \frac{k!\,\Gamma(k+q)\Gamma(k+p)\Gamma(k+p-q+1)}{(2k+p)\Gamma^2(2k+p)} \tag{47}$$

Any function $\Phi(z)$ in $0 < z < 1$ can be expanded with respect to the u_k in the form

$$\Phi(z) = \sum_{k=0}^{\infty} u_k(z) \int_0^1 dz'\, w(z')u_k(z')\Phi(z') \tag{48}$$

8. CONCLUSION

The equation of motion (6) for the time evolution of an ice cap has a similarity solution. The solution describes an ice cap of finite extent that grows in length and shrinks in height and is asymptotically stable with respect to all perturbations which leave the volume invariant.

Higher perturbation modes are damped strongly. Therefore, in practical calculations it will be sufficient to take only a few of the lowest modes into account.

APPENDIX 1

Consider the transformation

$$\eta = [1 + \varepsilon(\sigma, \xi)]\xi \qquad t = \sigma \tag{A1}$$

Its functional matrix is

$$\begin{bmatrix} \frac{\partial\sigma}{\partial t}, \frac{\partial\sigma}{\partial\eta} \\ \frac{\partial\xi}{\partial t}, \frac{\partial\xi}{\partial\eta} \end{bmatrix} = \frac{1}{(1+\partial/\partial\xi(\xi\varepsilon))} \begin{bmatrix} 1+\frac{\partial}{\partial\xi}(\xi\varepsilon), 0 \\ -\frac{\partial\varepsilon}{\partial\sigma}\xi, \quad 1 \end{bmatrix} \tag{A2}$$

The following condition guarantees the regularity of this transformation:

$$\left|\frac{\partial}{\partial\xi}(\xi\varepsilon)\right| < 1 \tag{A3}$$

From (A2) follows up to first order in ε:

$$\frac{\partial}{\partial t} = \frac{\partial}{\partial\sigma} - \xi\frac{\partial\varepsilon}{\partial\sigma}\frac{\partial}{\partial\xi} \tag{A4}$$

$$\frac{\partial}{\partial\eta} = \left[1 - \frac{\partial}{\partial\xi}(\xi\varepsilon)\right]\frac{\partial}{\partial\xi} \tag{A5}$$

Insertion of (A1), (A4), and (A5) and (29) into (27) gives the equation of linear perturbation theory for $\varepsilon(\sigma, \xi)$:

$$\sigma\frac{\partial}{\partial\sigma}[g(\xi) - \xi g'(\xi)]\,\varepsilon = \frac{-n}{3n+2}\frac{\partial}{\partial\xi}\left(\xi g(\xi)\varepsilon + \frac{\xi g(\xi)}{g'(\xi)} \cdot [g(\xi) - \xi g'(\xi)]\frac{\partial\varepsilon}{\partial\xi}\right) \tag{A6}$$

After division by $g - \xi g'$, one arrives at (30) with $\partial/\partial\sigma = \partial/\partial t$ at ξ fixed.

APPENDIX 2

To write (A6) in standard form, I use the transformations

$$z = \xi^{1+n/n} \qquad 0 < \xi < 1 \tag{A7}$$

$$\delta = \varepsilon(g - \xi g') = \frac{n}{2n+1}\left(\frac{2n+1}{n} - z\right)(1-z)^{(-n-1)/(2n+1)}\varepsilon \tag{A8}$$

Only the region $\xi > 0$ is considered. Owing to the symmetry $g(\xi) = g(-\xi)$, it will be clear how ε has to be continued into the region $\xi < 0$. The spectral parameter μ is defined through

$$\sigma\frac{\partial}{\partial\sigma}\delta = \mu\,\delta \tag{A9}$$

Then (A6) is equivalent to

$$0 = z(z-1)\frac{\partial^2\delta}{\partial z^2} + \left(\frac{(2n+1)^2 + (n+1)^2}{(2n+1)(n+1)}z - \frac{n}{n+1}\right)\frac{\partial\delta}{\partial z} + \left(\frac{n}{2n+1} + \frac{n(3n+2)}{(n+1)(2n+1)}\mu\right)\delta \tag{A10}$$

This is the Hypergeometric Differential Equation [*Smirnow*, 1970]. The condition (A3) means

$$\left|\frac{2n+1}{n}\left(1 + \frac{n+1}{n}z\frac{\partial}{\partial z}\right)\left(\frac{2n+1}{n} - z\right)^{-1}(1-z)^{(n+1)/(2n+1)}\delta\right| < 1 \tag{A11}$$

The roots of the corresponding fundamental equation at $z = 0, 1, \infty$, respectively, are

$$\alpha_1 = 0 \qquad \alpha_2 = \frac{1}{n+1} \tag{A12}$$

$$\beta_1 = 0 \qquad \beta_2 = -\frac{n+1}{2n+1} \tag{A13}$$

$$\gamma_{1,2} = \frac{3n^2+3n+1}{2(n+1)(2n+1)} \pm \frac{1}{2}\left(\left(\frac{3n^2+3n+1}{(n+1)(2n+1)}\right)^2 - 4\left(\frac{n(n+1) + n(3n+2)\mu}{(n+1)(2n+1)}\right)\right)^{1/2} \tag{A14}$$

and any solution of (A10) can be represented in the neighborhoods of $z = 0$ and $z = 1$ by

$$\delta = z^{\alpha_1}w_1(z) + z^{\alpha_2}w_2(z) \tag{A15}$$

$$\delta = (z-1)^{\beta_1}w_3(z) + (z-1)^{\beta_2}w_4(z) \tag{A16}$$

where the w_i are analytic at $z = 0,1$, respectively. The relations (A11), (A13), and (A16) imply

$$w_3 = 0 \tag{A17}$$

and from (A12) and (A15) one concludes

Symmetric case

$$w_2 = 0 \tag{A18}$$

Antisymmetric case

$$w_1 = 0 \tag{A19}$$

Therefore, $(z-1)^{-\beta_2}z^{-\alpha_1}\delta$ and $(z-1)^{-\beta_2}z^{-\alpha_2}\delta$ are analytic in the entire complex plane for the symmetric and antisymmetric case, respectively.

The set of solutions of (A10) is denoted by the symbol

$$P\begin{Bmatrix} 0 & 1 & \infty & \\ \alpha_1 & \beta_1 & \gamma_1 & z \\ \alpha_2 & \beta_2 & \gamma_2 & \end{Bmatrix} \tag{A20}$$

and in the sets [*Abramowitz and Stegun*, 1970]

Symmetric case

$$(z-1)^{-\beta_2}z^{-\alpha_1}P\begin{Bmatrix} 0 & 1 & \infty & \\ \alpha_1 & \beta_1 & \gamma_1 & z \\ \alpha_2 & \beta_2 & \gamma_2 & \end{Bmatrix} = P\begin{Bmatrix} 0 & 1 & \infty & \\ 0 & \beta_1 - \beta_2 & \gamma_1 + \alpha_1 + \beta_2 & z \\ \alpha_2 - \alpha_1 & 0 & \gamma_2 + \alpha_1 + \beta_2 & \end{Bmatrix} \tag{A21}$$

and

Antisymmetric case

$$(z-1)^{-\beta_2}z^{-\alpha_2}P\begin{Bmatrix} 0 & 1 & \infty & \\ \alpha_1 & \beta_1 & \gamma_1 & z \\ \alpha_2 & \beta_2 & \gamma_2 & \end{Bmatrix} = P\begin{Bmatrix} 0 & 1 & \infty & \\ \alpha_1 - \alpha_2 & \beta_1 - \beta_2 & \gamma_1 + \alpha_2 + \beta_2 & z \\ 0 & 0 & \gamma_2 + \alpha_2 + \beta_2 & \end{Bmatrix} \tag{A22}$$

one has to find an element which is analytic in the entire complex plane. The required functions are the Hypergeometric Functions $F(a, b, c; z)$ where [*Abramowitz and Stegun*, 1970]

Symmetric case

$$a, b = \gamma_{1,2} + \alpha_1 + \beta_2 \qquad c = 1 + \alpha_1 - \alpha_2 \tag{A23}$$

Antisymmetric case

$$a, b = \gamma_{1,2} + \alpha_2 + \beta_2 \qquad c = 1 - \alpha_1 + \alpha_2 \tag{A24}$$

and b (or a, notice the symmetry of the results in a,b) has to be a nonpositive integer $-k$, which means (cf. (A12)–(A14), (A23), and (A24))

Symmetric case

$$a = \frac{n^2 - n - 1}{(n + 1)(2n + 1)} + k \qquad b = -k \qquad c = \frac{n}{n + 1} \tag{A25}$$

Antisymmetric case

$$a = \frac{n^2 + 3n + 1}{(n + 1)(2n + 1)} + k \qquad b = -k \qquad c = \frac{n + 2}{n + 1} \tag{A26}$$

The eigenvalues μ are calculated from (A12)–(A14), (A23)–(A26) as

$$\mu_{s,k} = -\frac{(n + 1)(2n + 1)}{n(3n + 2)} k \left(k + \frac{n^2 - n - 1}{(n + 1)(2n + 1)}\right) \tag{A27}$$

$$\mu_{a,k} = -\frac{(n + 1)(2n + 1)}{n(3n + 2)} \left(k + \frac{n}{2n + 1}\right) \left(k + \frac{1}{n + 1}\right) \tag{A28}$$

Acknowledgment. I thank K. Hasselmann for his many criticisms and discussions. E. Maier-Reimer was also very helpful in my work with the computer.

REFERENCES

Abramowitz, M., and I. A. Stegun (Eds.), *Handbook of Mathematical Functions,* pp. 564, 777, 779, Dover, New York, 1970.

Andrews, J. T., *Glacial Systems,* p. 36, Duxbury, North Scituate, Mass., 1975.

Hays, J. D., J. Imbrie, N. J. Shackleton, Variations in the earth's orbit: Pacemaker of the ice ages, *Science, 194,* 1121, 1976.

Imbrie, J., and J. Z. Imbrie, Modelling the climatic response to orbital variations, *Science, 207,* 943, 1980.

Källén, E., C. Crafoord, and M. Ghil, Free oscillations in a climate model with ice sheet dynamics, *J. Atmos. Sci., 36,* 2292, 1979.

Mahaffy, M. W., A three-dimensional numerical model of ice sheets: Tests on the barnes ice cap, Northwest Territories, *J. Geophys. Res., 81,* 1059, 1976.

Nye, J. F., The mechanics of glacier flow, *J. Glaciol., 2,* 82, 1952.

Nye, J. F., The distribution of stress and velocity in glaciers and ice sheets, *Proc. R. Soc. London, Ser. A, 239,* 113, 1957.

Nye, J. F., Plasticity solution for a glacier snout, *J. Glaciol., 6,* 695, 1967.

Oerlemans, J., A simple model of stochastically driven ice sheet with planetary wave feedback, *Tellus, 31,* 469, 1979.

Paterson, W. S. B., *The Physics of Glaciers,* p. 195, Pergamon, New York, 1969.

Rooth, C. G. H., C. Emiliani, and H. W. Poor, Climate response to astronomical forcing, *Earth Planet. Sci. Lett., 41,* 387, 1978.

Smirnow, W. I., Lehrgang der höheren Mathematik, III/2, p. 316, VEB Deutscher Verlag d. Wiss., Berlin, 1970.

Weertman, J., Traveling waves on glaciers, paper presented at Chamonix Symposium, International Union of Geodesy and Geophysics, International Association of Scientific Hydrology, September 16–24, 1958.

Weertman, J., Rate of growth and shrinkage of nonequilibrium ice sheets, *J. Glaciol., 5,* 145, 1964.

(Received February 18, 1981;
revised July 6, 1981;
accepted July 7, 1981.)